Scientific Research Publishing

American Journal of Plant Sciences, 2022, 13, 1006-1022
https://www.scirp.org/journal/ajps
ISSN Online: 2158-2750
ISSN Print: 2158-2742

Uncovering Small RNAs in *Penicillium digitatum* by Transcriptome Sequencing

Pengcheng Zhang[1,2*], Qinru Yu[1*], Ran Li[1], Yaoyao Liu[1], Tongfei Lai[1#]

[1]College of Life and Environmental Science, Hangzhou Normal University, Hangzhou, China
[2]Worcester-Hangzhou Joint Molecular Plant Health Laboratory, School of Science and the Environment, University of Worcester, Worcester, UK
Email: [#]laitongfei@163.com

How to cite this paper: Zhang, P.C., Yu, Q.R., Li, R., Liu, Y.Y. and Lai, T.F. (2022) Uncovering Small RNAs in *Penicillium digitatum* by Transcriptome Sequencing. *American Journal of Plant Sciences*, **13**, 1006-1022.
https://doi.org/10.4236/ajps.2022.137067

Received: May 10, 2022
Accepted: July 22, 2022
Published: July 25, 2022

Abstract

Small RNAs in *Penicillium digitatum* were identified and analyzed via transcriptome sequencing on the BGISEQ-500 platform. A total of 15 predicted miRNAs and 10718 novel siRNAs were found. Their length distribution, sequence, predicted construction, base bias, expression levels and potential targets were determined as well. Through pathway and KEGG enrichment analysis, the miRNA target genes were mostly involved in carbohydrate metabolism, transport and catabolism, translation and amino acid metabolism. The target genes involved in aflatoxin biosynthesis and proteasome had a higher rich factor value. The results will provide a theoretical foundation for understanding the developmental and pathogenic mechanisms of *P. digitatum* at the transcriptional level.

Keywords

Penicillium digitatum, Transcriptome Sequencing, MicroRNA, Small Interfering RNA

1. Introduction

Penicillium digitatum belongs to the *Ascomycota* division and is the most economically important pathogen to the environment and the food industry, resulting in green mold disease in citrus fruits worldwide [1]. It can invade fruit through rind wounds during field harvesting, transport, packing, or other commercial treatment. After infection, the pathogen can quickly produce and accumulate spores on rotten fruit. Then, massive spores are airborne disseminated and can easily contaminate the surrounding hosts. Injury degree and maturity of

*Pengcheng Zhang and Qinru Yu contributed equally to this work.
#Corresponding author.

the fruit, temperature and the number of spores can determine the severity of the forthcoming disease development [2].

There are several factors that directly or indirectly mediate and affect the infection process of *P. digitatum.* To fight against the defense response of hosts, *P. digitatum* could increase the catalase accumulation to prevent oxidative bursts of hosts [3]. *P. digitatum* also could modulate the acidity of the environment, leading to an optimal condition for the degradation of the cell wall [4]. Meanwhile, *P. digitatum* could cause a necrotic reaction in the infected cells by producing small molecules, such as indole alkaloids tryptoquialanine, steroids cholesterol, ergosta, episterol and eburicol [5] [6]. However, the exact biological roles related to the pathogenicity of these secondary metabolites have not been illuminated yet. Through high-throughput sequencing and molecular techniques, a number of important genes involved in the infection process have been found [7]. These genes were conserved across the species and mostly belonged to transporters, cell wall-degrading enzymes, signaling pathway components and structural components. They generally influenced the pathogenicity of *P. digitatum* by affecting growth, asexual reproduction, cell wall integrity or the expression of other genes [8] [9] [10] [11].

So far, the conventional method for controlling this pathogen is the mass application of synthetic fungicides, such as fludioxonil, thiabendazole, pyrimethanil, prochloraz and imazalil, in citrus fruit [12]. However, the excessive usage of these fungicides has caused the development of resistant strains resulting in a breakdown of fungicide efficiency [13]. The toxicity of fungicides also leads to adverse effects on the environment and human health. The alternative management approaches for the control of *P. digitatum*, such as plant extracts and essential oils, salts, biocontrol agents, heat treatments, ionizing and non-ionizing irradiations and synthetic elicitors, have been investigated as well [14] [15]. Nevertheless, the molecular basis of the development, infection and specificity of the citrus hosts of *P. digitatum* remains largely unknown.

RNA has received extensive attention and it has been one of the most popular areas of life science research for nearly a decade. In eukaryotes, biological processes can be regulated through RNA-induced interference, which has in common the involvement of microRNAs (miRNAs) and small interfering RNAs (siRNAs). Most of the miRNAs can negatively regulate the expression of cellular mRNAs. Generally, pri-miRNA with a hairpin structure is firstly transcribed by RNA polymerase II in the nucleus and can be converted into pre-miRNA by RNase III type enzyme DROSHA and DGCR8 protein. Then, the pre-miRNA is transported into the cytoplasm by Exportin-5 and processed into miRNA duplex under RNase type III enzyme Dicer catalyzing. The miRNA duplex is incorporated in the RNA-induced silencing complex (RISC) together with Argonaute proteins (Ago) [16], where one strand becomes the mature miRNA [17]. The mature miRNA exerts its biological functions by spotting its complementary sequence in the 3'-untranslated region of the target mRNA [18] [19]. It is worth noting that a

single miRNA can recognize multiple mRNAs, and more than one miRNA can regulate the same target mRNA. The siRNA is a double-stranded RNA (dsRNA) of 20 - 25 nt. It originates from a long dsRNA generated by RNA-dependent RNA polymerase (RdRP). The dsRNA is cleaved into siRNA with two unpaired nucleotides at the 3'-end of each strand by RNase III-type Dicer ribonuclease. A guide strand is coupled with an Ago family protein to form RISC. The siRNA can lead RISC to target and cleave homologous mRNA [20] [21] [22]. However, the identification and biological function analysis of small RNAs in *P. digitatum* is less reported. In this study, small RNAs in *P. digitatum* were sequenced via high-throughput transcriptomic technology. The detected miRNAs and siRNAs were characterized and target genes of miRNAs were predicted. The results will provide a theoretical foundation for understanding pathogenic genes and regulatory pathways of *P. digitatum* at the transcriptional level.

2. Materials and Methods

2.1. Fungal Identification and Phenotype

P. digitatum was isolated from a naturally infected *Citrus sinensis* (L.) Osbeck fruit with a typical green mold symptom, and maintained on potato dextrose agar (PDA) medium at 25˚C. The phenotype of spores and mycelia was microscopically observed using a Nikon Eclipse Ni-U microscope (Nikon, Japan). To confirm the genetic background of fungus, total DNA was isolated using a DNeasy Plant Mini kit, following the manufacturer's instructions. The rDNA-ITS was amplified using universal primers ITS4 (5'-TCCTCCGCTTATTGATATGC-3') and ITS5 (5'-GGAAGGTAAAAGTCGTAACAAG-3'). PCR reactions were conducted in a total volume of 20 μL containing 0.2 μL Primerstar HS DNA polymerase (2.5 unit/μL), 4 μL 5 × Buffer, 1 μL dNTP (2.5 mmol/L), 1 μL primer each (10 μmol/L), 0.8 μL genome DNA (about 20 ng), and 12 μL ddH_2O. Amplification conditions were 94˚C for 5 min followed by 30 cycles of 94˚C for 30 s, 58˚C for 30 s, and 72˚C for 1 min, then 72˚C for 10 min. Amplified products were extracted, purified and sequenced by Sangon Biotech (Shanghai) Co., Ltd. The sequence was analyzed in http://blast.ncbi.nlm.nih.gov/Blast.cgi.

2.2. Small RNA Sequencing

Fresh spores of *P. digitatum* were prepared by flooding the sporulating cultures of *P. digitatum* with sterile water containing 0.05% Tween-20. The suitable spore suspension was added into 100 mL potato dextrose broth (PDB) and the final concentration was 1×10^6 spores/mL. After 24 h of culture at 25˚C under shaking conditions, the spores and mycelia were harvested by centrifugation, washed twice with sterile distilled water, and quickly frozen in liquid nitrogen. A biological repeat was performed and both samples were mixed with equal weight. The technology service of small RNA sequencing was provided by Beijing Genomics Institute (BGI) Co., Ltd. Briefly, small RNA was separated from total RNA by

PAGE gel, and linked with a 5'-adenylated, 3'-blocked single-stranded DNA adapter at the 3' end. After RT primer hybridization, the 5'-adaptor was linked and the first-strand of cDNA was synthesized. To enrich cDNA of 100 - 120 bp, PCR amplification and PAGE gel separation were carried out. Finally, the library was quantified and pooling cyclization was performed. Each step was under strict quality control. Then, the transcriptome sequencing was performed using the BGISEQ-500 platform.

2.3. Bioinformatic Analysis

The bioinformatics pipeline is as followed. The original data were removed adaptors, low-quality reads and other contaminants to acquire clean reads. Then, the remaining clean tags (clean reads) were converted into FASTQ format. For small RNA annotation, Bowtie2 and Cmsearch were used to map clean reads to the reference genome, other sRNAs or Rfam [23] [24]. The priority rule of the small RNA classification was as followed: MiRbase > pirnabank > snoRNA > Rfam > other sRNAs. miRDeep2 and miRA were used to predict novel miRNA based on the characteristic hairpin structure of the miRNA precursor [25] [26]. The standard of siRNA predicting was that siRNA was a 22 - 24 nt dsRNA, each strand of which was 2 nt longer than the other [27]. The small RNA expression level was calculated by using TPM (transcripts per million). TPM = $C \times 10^4/N$. C means miRNA counts number in a sample, and N means total reads number that mapped to the genome [28]. TAPIR was used to predict miRNA target genes and the default parameters were score 5 and mfe_ratio 0.6 [29]. KEGG database was used to perform pathway enrichment analysis of miRNA target genes. A scatter plot and a bar plot of KEGG enrichment analysis were generated. A corrected *P* value ≤ 0.05 was taken as a threshold.

3. Results

3.1. Phenotype and Genetic Background of *P. digitatum*

The pathogen was demonstrated as the main pathogen of citrus fruit through an artificial infection and it was highly pathogenic. Disease incidence of fruit after inoculation of *P. digitatum* reached 100% within 72 h. After 7 days, lesions were water-stained and pale brown. The hyphae gradually extended on the surface of the pericarp with vague and irregular edges. A green mold layer with massive spores was formed, and the whole fruit was observed to rot and soften (**Figure 1(A)**). On the PDA plate, colonies with white margins were green and numerous green spores are covered on the surface (**Figure 1(B)**). The reverse of colonies was colorless to pale brown. Conidiophores were verticillate, irregularly branched and composed of short stipes with few metulae. Conidia without septum are round or elliptical (**Figure 1(C)**). After amplification using ITS universal primers, a product with 584 bp in length was obtained (**Figure 1(D)** and **Figure 1(E)**). Through sequencing and megablast analysis, the sequence of the product perfectly matched with partial ribosomal RNA gene of the *P. digitatum* strains

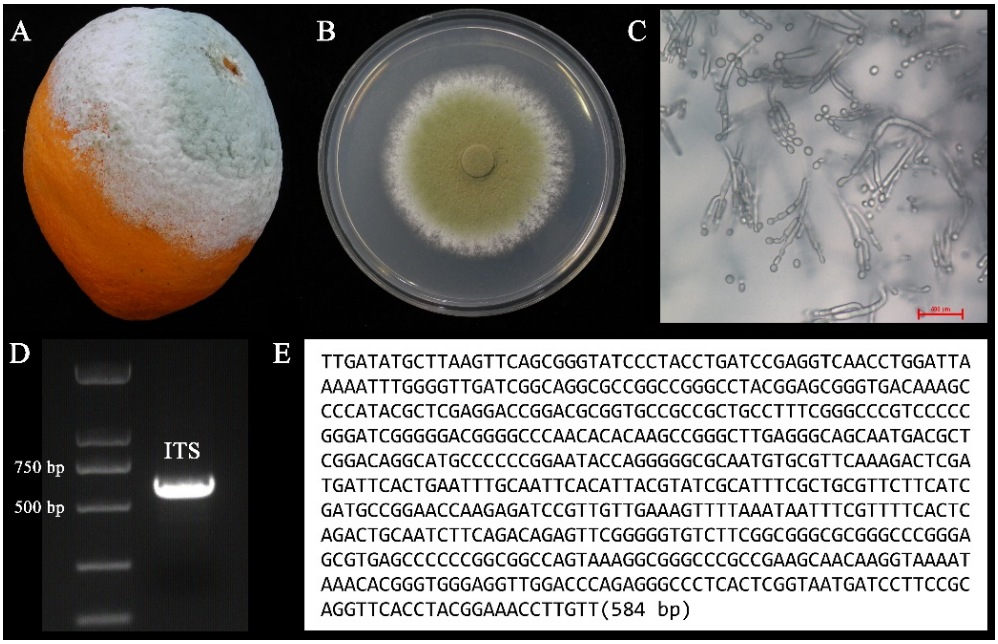

Figure 1. The phenotype and rDNA-ITS molecular character of *Penicillium digitatum*. (A) The symptom of *Penicillium digitatum* on *Citrus sinensis* (L.) Osbeck; (B) The colonial phenotype of *Penicillium digitatum* on PDA plate; (C) The spores and mycelia phenotype of *Penicillium digitatum*; (D) The amplified product using ITS universal primers; (E) Sequence of the target fragment.

CMV010G4, CBS128276, IPBCC.16.1354, etc. According to morphological and molecular characteristics, the fungus, which exhibited a normal growth status and pathogenicity, was confirmed as *P. digitatum* and used in the sequent experiments.

3.2. Small RNA Sequencing Results

After sequencing by BGISEQ-500 system, a total of 28352228 raw tags containing 295220 short valid length tags, 1575 polyA tags, 352675 low-quality tags, 879926 invalid adapter tags, and 26822832 clean tags were acquired. The length of small RNAs was in a range of 10 - 44 nt, and the number of small RNAs in a range of 19 - 23 nt was the largest (**Figure 2(A)**). The base percentage composition of clean tags was shown in **Figure 2(B)**. The percentage of clean tags, of which quality was more than 20, was 98.80% (**Figure 2(C)**). The percentage of clean tags, which were aligned to the reference genome, was 74.57%. Among them, 85300 Rfam other sncRNAs, 2208 snRNAs, 104407 rRNAs, 2628 snoRNAs, 3423 precursors, and 939 tRNAs were annotated. The genome distribution of tags was shown in **Figure 3(A)** and the proportion of all kinds of sRNAs was shown in **Figure 3(B)**.

3.3. Prediction of miRNAs and siRNAs

Only miR-190-5p-1 as known miRNA was found in *P. digitatum.* Fifteen novel miRNAs named as Pdmir1 to Pdmir15 were predicted. Their expression levels were significantly different, of which the TMP values ranged from 0.38 to 2735.

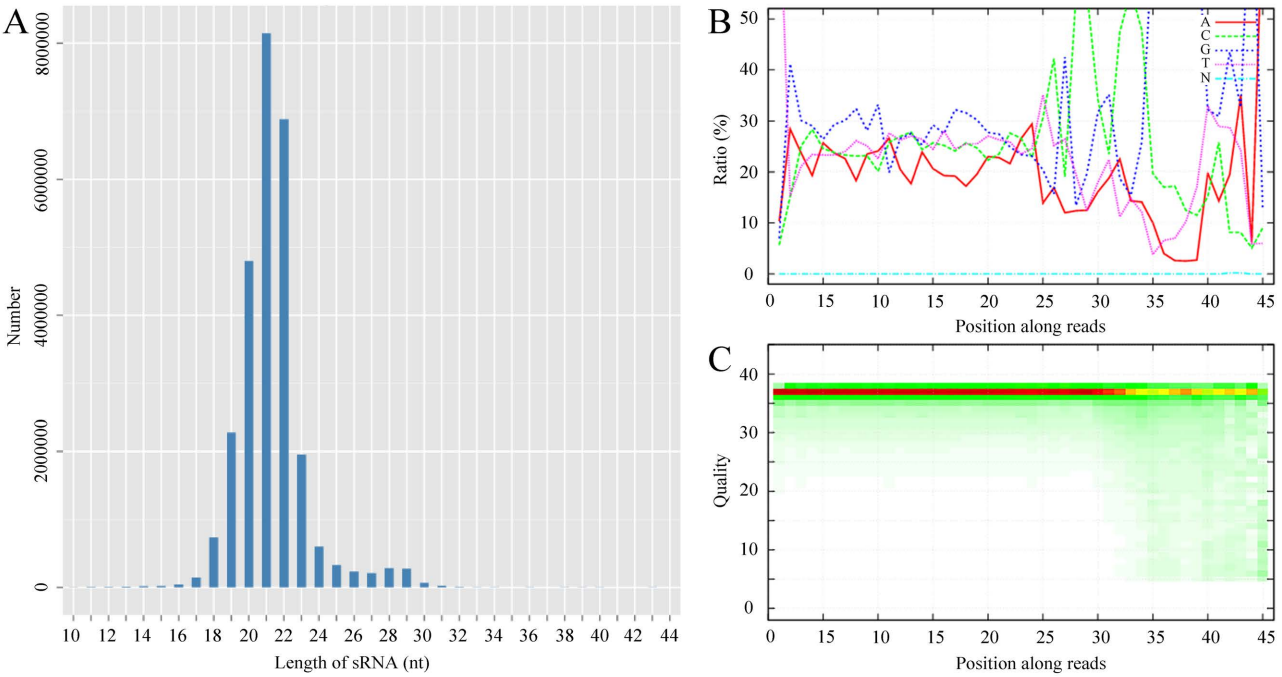

Figure 2. Distribution length, base, base quality of small RNAs in *Penicillium digitatum*. (A) Length distribution of small RNAs; (B) Base distribution of small RNAs; (C) Base quality distribution on the clean tag. Each dot represents the total number of bases with a specific quality value of the corresponding base along a tag, and darker color indicates higher base number.

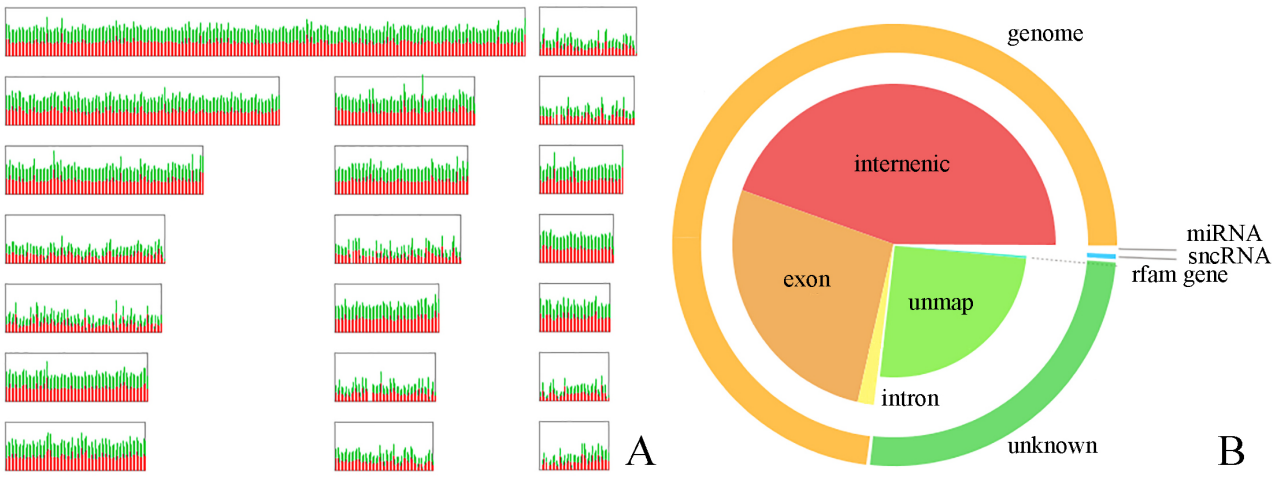

Figure 3. Genome and catalog distribution of small RNAs. (A) Catalog distribution of tags. The X-axis shows the relative position in the chromosome, and the Y-axis shows the number of tags. The red represents tag count, whereas green represents tag catalogs; (B) The ratio of different types of small RNA.

The detailed information of novel miRNAs was shown in Table 1. The stem-loop structure of precursors was shown in Figure 4. A total of 10718 novel siRNAs were predicted based on their architectural feathers. The details of novel siRNAs were shown in Table S1. Their expression levels were represented by the TPM values in a range of 0.38 to 2296. Through sequence analysis, the base composition of predicted miRNAs and siRNAs was shown in Figure 5. For novel miRNAs, the base distribution between them was significantly different. Four kinds

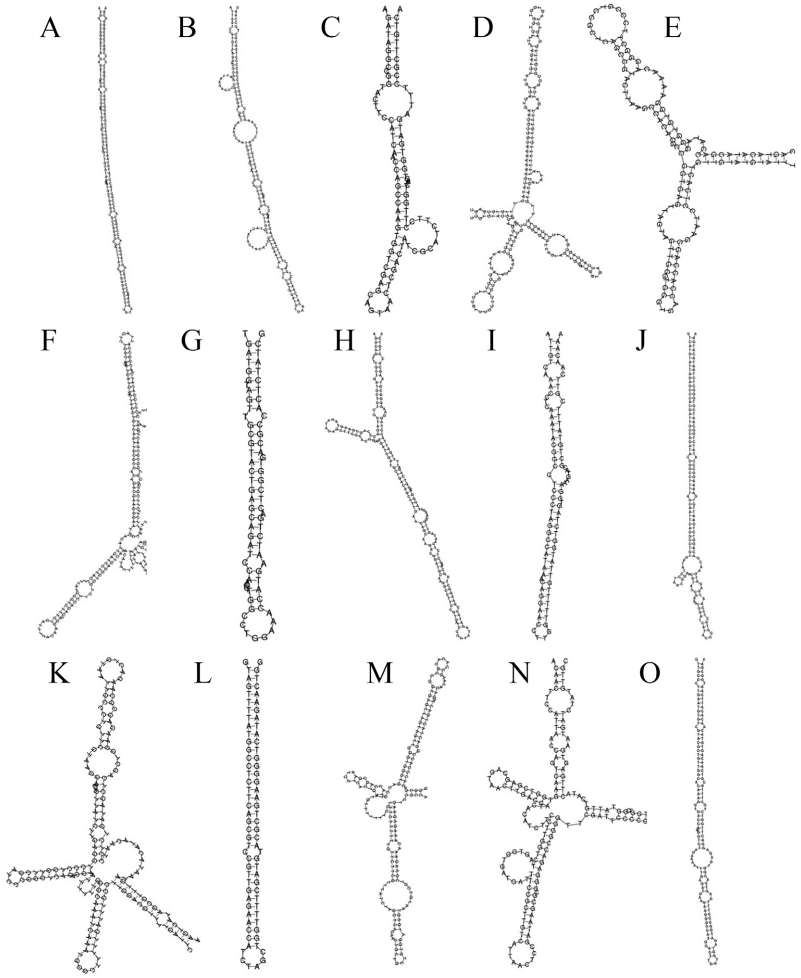

Figure 4. Stem-loop structure of predicted novel miRNA precursor in *Penicillium digitatum*. (A) to (O) indicate the predicted miRNAs named as Pdmir1 to Pdmir15.

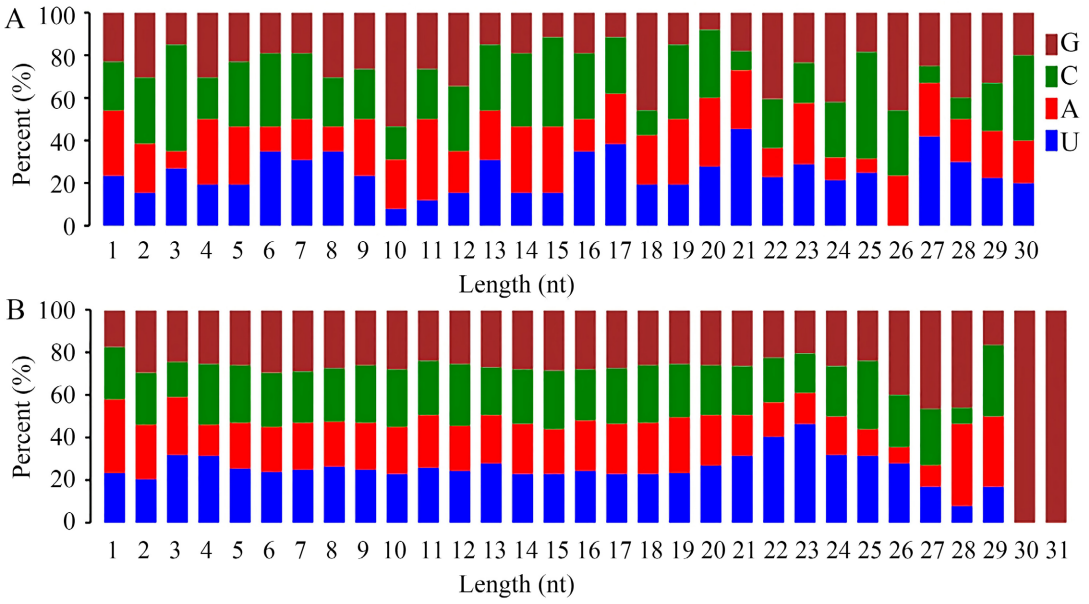

Figure 5. The base distribution in predicted miRNAs (A) and siRNAs (B) in *Penicillium digitatum*.

Table 1. Information of predicted miRNAs in *Penicillium digitatum*.

Name	Chromosome	Strand	TPM	Sequence (mature)
Pdmir1	AYHP01000300.1	+	40.71	CGCGACTGTGGCTGCGTTGCGTTGCATAGA
Pdmir2	AYHP01000330.1	+	1.49	ACCAATCGCGAGCAATCGCACCTCTGATC
Pdmir3	AYHP01000412.1	+	2735.09	GGTACTTCCATCAACCAGCCAAGTGG
Pdmir4	AYHP01000424.1	+	1318.92	GACCACCAGCGAATCCTCACTGTTG
Pdmir5	AYHP01000425.1	+	27.08	AGGGTGTGGAAAACAGGGCTTCCC
Pdmir6	AYHP01000480.1	+	2.41	GTGCGGCGGCGCAACTCGATAAC
Pdmir7	AYHP01000520.1	+	16.58	TACTGAGCAGATCCAACCTTGGCCTGG
Pdmir8	NW_014574581.1	+	107.13	AGCAAGACGGATGCAAGGCC
Pdmir9	NW_014574583.1	+	378.76	GCCTCCCTAGGCCATAAACAGGAA
Pdmir10	NW_014574584.1	+	136.12	TATTAGAGCCCACGATTGCCAGATA
Pdmir11	NW_014574585.1	+	94.53	CCTCTGATAGCTCAGCTGGAAGAGC
Pdmir12	NW_014574590.1	+	26.08	GCGTCCGTTGAGAACCATC
Pdmir13	NW_014574590.1	+	0.38	CACGCCGGTGAGTTAGTAGTTGGGTGGGT
Pdmir14	NW_014574616.1	+	25.7	CTTGGTCTAGTGGTGATGATTTCCGCTTGT
Pdmir15	NW_014574621.1	+	47.53	TGTCGTACGCTGTTGGCACAAAGG

of bases were almost distributed evenly in the length range of 1 to 20 nt of novel siRNAs. Whereas, the percent of base A was less than other bases in the length range of 21 to 27 nt of novel siRNAs. The first base distribution of predicted miRNAs and siRNAs was shown in Figure 6. For novel miRNAs, there were no obvious rules for the base distribution due to the small number. For novel siRNAs, the first base distribution was A, U, C and G in numbers from high to low. In addition, the first base did not contain bases U and C, when the length of siRNAs was longer than 27 nt.

3.4. Enrichment Analysis of miRNA Target Genes

Software TAPIR was used to find the target genes of miRNAs in *P. digitatum*, and the detailed information was shown in Table S2. A total of 37 targets for 6 novel miRNAs (Pdmir4, Pdmir5, Pdmir6, Pdmir8, Pdmir12 and Pdmir13) were predicted. Among them, Pdmir8 and Pdmir12 have 14 and 18 possible targets, respectively. These target genes encoded many proteins with different biological functions, such as Acetyl-coenzyme A carboxyltransferase, Mycocerosic acid synthase, Amino acid/polyamine transporter, Ubiquitin-protein ligase, Lipase, BZIP transcription factor, Protein kinase, ATPase, etc. Statistics of pathway enrichment indicated that many target genes were related to the ribosome, proteasome, MAPK signaling pathway, endocytosis, amino sugar and nucleotide sugar metabolism, and aflatoxin biosynthesis. Meanwhile, target genes involved in aflatoxin biosynthesis and proteasome possessed higher rich factor values (Figure 7). The KEGG enrichment result was shown in Figure 8. The items with a larger

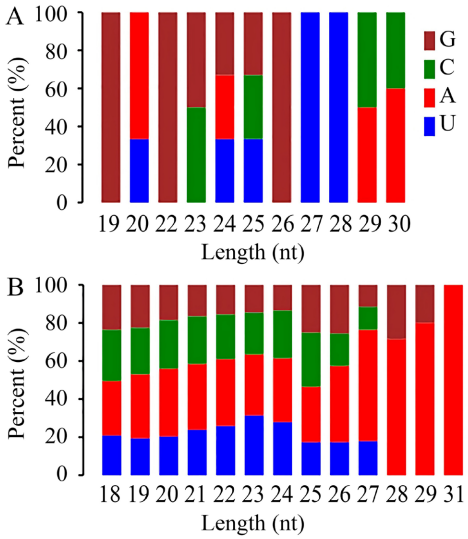

Figure 6. The first base distribution of predicted miRNAs (A) and siRNAs (B) in *Penicillium digitatum.*

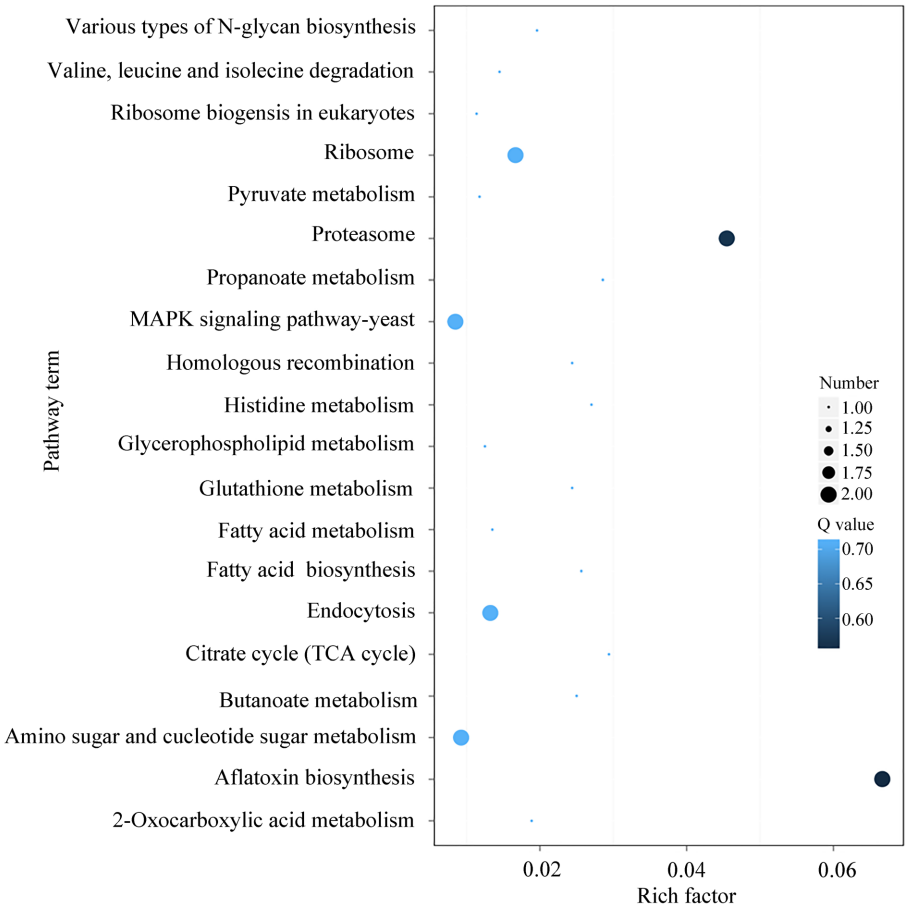

Figure 7. Pathway enrichment analysis of miRNA target genes in *Penicillium digitatum*. The rich factor is the ratio of target gene numbers annotated in this pathway term to all gene numbers annotated in this pathway term. Greater rich factor indicates greater degree of enrichment. The Q-value is the corrected *P*-value, and the lower Q-value indicates the greater enrichment level.

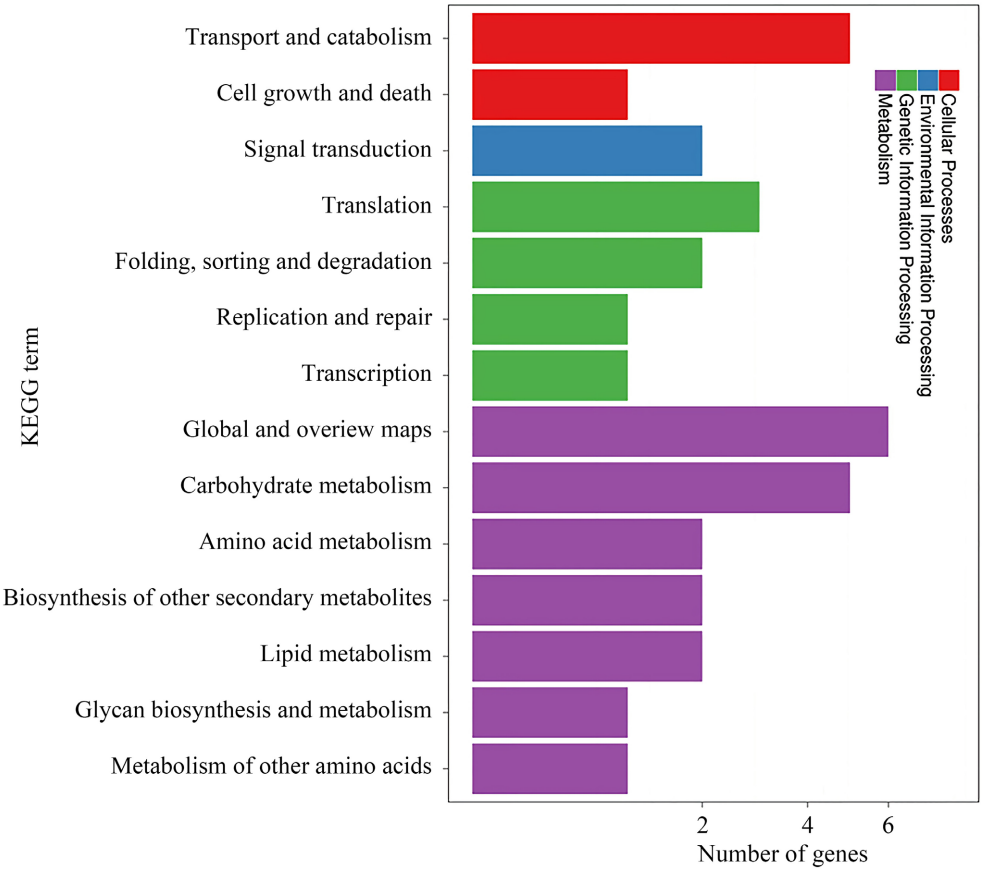

Figure 8. KEGG enrichment statistics of miRNA target genes in *Penicillium digitatum*. The X axis means the number of target genes, the Y-axis shows the second KEGG pathway terms and the first pathway terms are indicated using different colors.

number of target genes were carbohydrate metabolism, translation, and transport and catabolism.

4. Discussion

Generally, RNA interference (RNAi) is induced by non-coding small RNAs which are produced by endoribonucleases loaded into Ago proteins or Dicer-like proteins [30]. Depending on the morphology and biosynthetic pathways, small RNAs can be divided into 2 groups miRNAs and siRNAs. Both of these small RNAs are involved in complex cellular mechanisms, developmental processes and genetic expression regulations [31] [32]. In addition, systemic intracellular signal transformation by small RNAs is at a considerable long distance and can induce the particular phenomena in cells [33]. For fungal pathogens, these small RNAs may play an active part in the development of offensive strategies and pathogenesis [34]. *Mangnoporthe oryzae* embeds several sRNAs in appressoria which can help to infect *Oryzae sativa* [35]. *Botrytis cinerea* can incorporate a particular class of small RNAs to capture the host RNA interfering machinery leading to suppression of immunity responsive genes of host [36] [37] [38]. *Phytophthora namorum*, *Phytophthora infestans* and *Phytophthoras sojae*

can produce certain miRNAs and siRNAs during the introduction of infection [39]. Furthermore, Pst-milR1 in *Puccinia striiformis* f. sp. tritici could suppress host immunity [40]. The miR8788 acted as an important pathogenicity factor to facilitate the infection of *Phytophthora infestans* [41]. A 23-nucleotide siRNA based on the *ornithine decarboxylase* gene played an important role in mycelial development and polyamine biosynthesis [42]. In this study, miR-190-5p as a known miRNA was found in *P. digitatum*. Although little was known about the role of miR-190-5p in fungi, accumulating evidences indicated that miR-190-5p could play multiple roles in human diseases, notably in cancer, drug addiction, pulmonary arterial hypertension and diabetes mellitus [43] [44] [45]. Its target genes were closely associated with cellular proliferation, apoptosis, metastasis, and drug resistance [46]. From these scientific and convincing studies, we assumed that miR-190-5p also functioned as an important factor in development and pathogenicity of *P. digitatum*. Additionally, we disclosed that the novel miRNAs of *P. digitatum* had a diverse range of target genes, which were mostly involved in carbohydrate metabolism, translation, and transport and catabolism. They contributed to the fungal development and progress via complicated and variable molecular mechanisms that need to be investigated in future.

Considering the multiple biological functions of small RNAs in fungi, the exploration of novel miRNAs and siRNAs is becoming more important [47]. This study is devoted to finding small RNAs and the predicted targets of miRNAs in *P. digitatum.* Although the exact biological functions of these small RNAs are not clear, the findings will help to understand the small RNA transcriptome and provide new insights into miRNAs' function in *P. digitatum.*

5. Conclusion

In this study, a total of 15 novel miRNAs and 10718 novel siRNAs in *P. digitatum* were predicted through high-throughput transcriptomic sequencing. The sequences, base distribution, expression level and possible targets of these small RNAs were also determined. In addition, KEGG and pathway enrichment analysis indicated that the miRNA target genes were mostly involved in carbohydrate metabolism, translation, and transport and catabolism. These results will provide new clues to uncovering the developmental and pathogenic mechanisms of *P. digitatum* at the transcriptional level.

Acknowledgements

This research was financially supported by the Scientific Research Fund of the Zhejiang Provincial Education Department (Y202044822) and the Zhejiang Provincial Natural Science Foundation of China (LY22C150009).

Conflicts of Interest

The authors declare no conflicts of interest regarding the publication of this paper.

References

[1] Ghooshkhaneh, N.G., Golzarian, M.R. and Mamarabadi, M. (2018) Detection and Classification of Citrus Green Mold Caused by *Penicillium digitatum* Using Multispectral Imaging. *Journal of the Science of Food and Agriculture*, **98**, 3542-3550. https://doi.org/10.1002/jsfa.8865

[2] Costa, J.H., Bazioli J.M., Pontes, J.G.D.M. and Fill T.P. (2019) *Penicillium digitatum* Infection Mechanisms in Citrus: What Do We Know So Far? *Fungal Biology*, **123**, 584-593. https://doi.org/10.1016/j.funbio.2019.05.004

[3] Macarisin, D., Cohen, L., Eick, A., Rafael, G., Belausov, E., Wisniewski, M. and Droby, S. (2007) *Penicillium digitatum* Suppresses Production of Hydrogen Peroxide in Host Tissue during Infection of Citrus Fruit. *Phytopathology*, **97**, 1491-1500. https://doi.org/10.1094/PHYTO-97-11-1491

[4] Prusky, D., McEvoy, J.L., Saftner, R., Conway, W.S. and Jones R. (2004) Relationship between Host Acidification and Virulence of Penicillium spp. on Apple and Citrus Fruit. *Phytopathology*, **94**, 44-51. https://doi.org/10.1094/PHYTO.2004.94.1.44

[5] Ariza, M.R., Larsen T.O., Petersen, B.O., Duus, J.Ø. and Barrero, A.F. (2002) *Penicillium digitatum* Metabolites on Synthetic Media and Citrus Fruits. *Journal of Agricultural and Food Chemistry*, **50**, 6361-6365. https://doi.org/10.1021/jf020398d

[6] Costa, J.H., Bazioli, J.M., Araújo E.D.V., Vendramini, P.H., Porto, M.C.D.F., Eberlin, M.N., Souza-Neto, J.A. and Fill, T.P. (2019) Monitoring Indole Alkaloid Production by *Penicillium digitatum* during Infection Process in Citrus by Mass Spectrometry Imaging and Molecular Networking. *Fungal Biology*, **123**, 594-600. https://doi.org/10.1016/j.funbio.2019.03.002

[7] Marcet-Houben, M., Ballester, A., Fuente, B.D.L., Harries, E., Marcos, J., González-Candelas, L. and Gabaldón, T. (2012) Genome Sequence of the Necrotrophic Fungus *Penicillium digitatum*, the Main Postharvest Pathogen of Citrus. *BMC Genomics*, **13**, Article No. 646. https://doi.org/10.1186/1471-2164-13-646

[8] Sun, X.P., Ruan, R.X., Lin, L.Y., Zhu, C.Y., Zhang, T.Y., Wang, M.S., Li, H.Y. and Yu, D.L. (2013) Genomewide Investigation into DNA Elements and ABC Transporters Involved in Imazalil Resistance in *Penicillium digitatum*. *FEMS Microbiology Letters*, **348**, 11-18. https://doi.org/10.1111/1574-6968.12235

[9] Julca, I., Droby, S., Sela, N., Marcet-Houben, M. and Gabaldón T. (2015) Contrasting Genomic Diversity in Two Closely Related Postharvest Pathogens: *Penicillium digitatum* and *Penicillium expasum*. *Genome Biology and Evolution*, **8**, 218-227. https://doi.org/10.1093/gbe/evv252

[10] Zhu, C.Y., Sheng, D.L., Wu, X.D., Wang, M.S., Hu, X., Li, H.Y. and Yu, D.L. (2017) Identification of Secondary Metabolite Biosynthetic Gene Clusters Associated with the Infection of Citrus Fruit by *Penicillium digitatum*. *Postharvest Biology and Technology*, **134**, 17-21. https://doi.org/10.1016/j.postharvbio.2017.07.011

[11] Vu, T.X., Ngo, T.T., Mai, L.T.D., Bui, T., Le, D.H., Bui, H.T.V., Nguye, H.Q., Ngo, B.X. and Tran, V. (2018) A Highly Efficient *Agrobacterium tumefaciens*-Mediated Transformation System for the Postharvest Pathogen *Penicillium digitatum* Using DsRed and GFP to Visualize Citrus Host Colonization. *Journal of Microbiological Methods*, **144**, 134-144. https://doi.org/10.1016/j.mimet.2017.11.019

[12] Hao, W.N., Li, H., Hu, M.Y., Yang, L. and Rizwan-ul-Haq, M. (2011) Integrated Control of Citrus Green and Blue Mold and Sour Rot by *Bacillus amyloliquefaciens* in Combination with Tea Saponin. *Postharvest Biology and Technology*, **59**, 316-323. https://doi.org/10.1016/j.postharvbio.2010.10.002

[13] Kanetis, L., Förster, H. and Adaskaveg, J.E. (2010) Determination of Natural Resistance Frequencies in *Penicillium digitatum* Using a New Air-Sampling Method and Characterization of Fludioxonil- and Pyrimethanil-Resistant Isolates. *Phytopathology*, **100**, 738-746. https://doi.org/10.1094/PHYTO-100-8-0738

[14] Papoutsis K, Mathioudakis, M.M., Hasperué, J.H. and Ziogas, V. (2019) Non-Chemical Treatments for Preventing the Postharvest Fungal Rotting of Citrus Caused by *Penicillium digitatum* (Green Mold) and *Penicillium italicum* (Blue Mold). *Trends in Food Science & Technology*, **86**, 479-491. https://doi.org/10.1016/j.tifs.2019.02.053

[15] Bhatta, U.K. (2022) Alternative Management Approaches of Citrus Disease Caused by *Penicillium digitatum* (Green Mold) and *Penicillium italicum* (Blue Mold). *Frontiers in Plant Science*, **12**, Article ID: 833328. https://doi.org/10.3389/fpls.2021.833328

[16] Azlan, A., Dzaki, N. and Azzam, G. (2016) Argonaute: The Executor of Small RNA Function. *Journal of Genetics and Genomics*, **43**, 481-494. https://doi.org/10.1016/j.jgg.2016.06.002

[17] Yadav, A., Sanyal, I., Rai, S.P. and Lata, C. (2021) An Overview on MiRNA-Encoded Peptides in Plant Biology Research. *Genomics*, **113**, 2385-2391. https://doi.org/10.1016/j.ygeno.2021.05.013

[18] Jonas, S. and Izaurralde, E. (2015) Towards a Molecular Understanding of MicroRNA-Mediated Gene Silencing. *Nature Review Genetics*, **16**, 421-433. https://doi.org/10.1038/nrg3965

[19] Iwakawa, H.O. and Tomari, Y. (2015) The Functions of MicroRNAs: mRNA Decay and Translational Repression. *Trends in Cell Biology*, **25**, 651-665. https://doi.org/10.1016/j.tcb.2015.07.011

[20] Meister, G. and Tuschl, M. (2004) Mechanisms of Gene Silencing by Double-Stranded RNA. *Nature*, **431**, 343-349. https://doi.org/10.1038/nature02873

[21] Jinek, M. and Doudna, J.A. (2009) A Three-Dimensional View of the Molecular Machinery of RNA Interference. *Nature*, **457**, 405-412. https://doi.org/10.1038/nature07755

[22] Meister, G. (2013) Argonaute Proteins: Functional Insights and Emerging Roles. *Nature*, **14**, 864-872. https://doi.org/10.1038/nrg3462

[23] Langmead, B., Trapnell, C., Pop, M. and Salzberg, S.L. (2009) Ultrafast and Memory-Efficient Alignment of Short DNA Sequences to the Human Genome. *Genome Biology*, **10**, Article No. R23. https://doi.org/10.1186/gb-2009-10-3-r25

[24] Nawrocki, E.P. and Eddy, S.R. (2013) Infernal 1.1: 100-Fold Faster RNA Homology Searches. *Bioinformatics*, **29**, 2933-2935. https://doi.org/10.1093/bioinformatics/btt509

[25] Friedländer, M.R., Chen, W., Adamidi, C., Maaskola, J., Einspanier, R., Knespel, S. and Rajewsky, N. (2008) Discovering MicroRNAs from Deep Sequencing Data Using MiRDeep. *Nature Biotechnology*, **26**, 407-415. https://doi.org/10.1093/bioinformatics/btt509

[26] Evers, M., Huttner, M., Dueck, A., Meister, G. and Engelmann, J.C. (2015) MiRA: Adaptable Novel MiRNA Identification in Plants Using Small RNA Sequencing Data. *BMC Bioinformatics*, **16**, Article No. 370. https://doi.org/10.1186/s12859-015-0798-3

[27] Jagla, B., Aulner, N., Kelly, P.D., Song, D., Volchuk, A., Zatorski, A., Shum, D., Mayer, T., De Angelis, D.A., Ouerfelli, O., Rutishauser, U. and Rothman, J.E. (2005) Sequence Characteristics of Functional SiRNAs. *RNA*, **11**, 864-872. https://doi.org/10.1261/rna.7275905

[28] Hoen, P.A.C., Ariyurek, Y., Thygesen, H.H., Vreugdenhil, E., Vossen, R.H.A.M., De Menezes, R.X., Boer, J.M., Van Ommen, G.B. and Den Dunnen, J.T. (2008) Deep Sequencing-Based Expression Analysis Shows Major Advances in Robustness, Resolution and Inter-Lab Portability over Five Microarray Plat Forms. *Nucleic Acids Research*, **36**, e141. https://doi.org/10.1093/nar/gkn705

[29] Bonnet, E., He, Y., Billiau, K. and De Peer, Y.V. (2010) TAPIR, a Web Server for the Prediction of Plant MicroRNA Targets, Including Target Mimics. *Bioinformatics*, **26**, 1566-1568. https://doi.org/10.1093/bioinformatics/btq233

[30] Borges, F. and Martienssen, R.A. (2015) The Expanding World of Small RNAs in Plants. *Nature Reviews Molecular Cell Biology*, **16**, 727-741. https://doi.org/10.1038/nrm4085

[31] Castel, S.E. and Martienssen, R.A. (2013) RNA Interference (RNAi) in the Nucleus: Roles for Small RNA in Transcription, Epigenetics and Beyond. *Nature Reviews Genetics*, **14**, 100-112. https://doi.org/10.1038/nrg3355

[32] Weiberg, A., Bellinger, M. and Jin, H.L. (2015) Conversations between Kingdoms: Small RNAs. *Current Opinion in Biotechnology*, **32**, 207-215. https://doi.org/10.1016/j.copbio.2014.12.025

[33] Hisanaga, T., Miyashima, S. and Nakajima, K. (2014) Small RNAs as Positional Signal for Pattern Formation. *Current Opinion in Plant Biology*, **31**, 37-42. https://doi.org/10.1016/j.pbi.2014.06.005

[34] Islam, W., Islam, S.U., Qasim, M. and Wang, L.D. (2017) Host-Pathogen Interactions Modulated by Small RNAs. *RNA Biology*, **7**, 891-904. https://doi.org/10.1080/15476286.2017.1318009

[35] Nunes, C.C., Gowda M., Sailsbery, J., Xue, M.F., Chen, F., Brown, D.E., Oh, Y.Y., Mitchell, T.K. and Dean, R.A. (2011) Diverse and Tissue-Enriched Small RNAs in the Plant Pathogenic Fungus, *Magnaporthe oryzae*. *BMC Genomics*, **12**, Article No. 288. http://www.biomedcentral.com/1471-2164/12/288 https://doi.org/10.1186/1471-2164-12-288

[36] Weiberg, A, Wang, M., Lin, F.M., Zhao, H.W., Zhang, Z.H., Kaloshian, I., Huang, H.D. and Jin, H.L. (2013) Fungal Small RNAs Suppress Plant Immunity by Hijacking Host RNA Interference Pathways. *Science*, **342**, 118-123. https://doi.org/10.1126/science.1239705

[37] Weiberg, A. and Jin, H.L. (2015) Small RNAs—The Secret Agents in the Plant-Pathogen Interactions. *Current Opinion in Plant Biology*, **26**, 87-94. https://doi.org/10.1016/j.pbi.2015.05.033

[38] Ye, R.Q., Chen, Z.L., Lian, B., Rowley, M.J., Xia, N., Chai, J.J., Li, Y., He, X.J., Wierzbicki, A.T. and Qi, Y.J. (2016) A Dicer-Independent Route for Biogenesis of SiRNAs That Direct DNA Methylation in Arabidopsis. *Molecular Cell*, **61**, 222-235. https://doi.org/10.1016/j.molcel.2015.11.015

[39] Fahlgren, N., Bollmann, S.R., Kasschau, K.D., Cuperus, J.T., Press, C.M., Sullivan, C.M., Chapman, E.J., Hoyer, J.S., Gilbert, K.B., Grünwald, N.J. and Carrington, J.C. (2013) Phytophthora Have Distinct Endogenous Small RNA Populations That Include Short Interfering and MircroRNAs. *PLOS ONE*, **8**, e77181. https://doi.org/10.1371/journal.pone.0077181

[40] Wang, B., Sun, Y.F., Song, N., Zhao, M.X., Liu, R., Feng, H., Wang, X.J. and Kang, Z.S. (2017) *Puccinia striiformis* f. sp. *tritici* MicroRNA-Like RNA 1 (Pst-milR1), an Important Pathogenicity Factor of *Pst*, Impairs Wheat Resistance to *Pst* by Suppressing the Wheat Pathogenesis-Related 2 Gene. *New Phytologist*, **215**, 338-350. https://doi.org/10.1111/nph.14577

[41] Hu, X.Y., Hoden, K.P., Liao, Z., Asman, A. and Dixelius, C. (2022) *Phytophthora infestans* Ago1-Associated MiRNA Promotes Potato Late Blight Disease. *New Phytologist*, **233**, 443-457. https://doi.org/10.1111/nph.17758

[42] Khatri, M. and Rajam, M.V. (2007) Targeting Polyamines of *Aspergillus nidulans* by SiRNA Specific to Fungal Ornithine Decarboxylase Gene. *Medical Mycology*, **45**, 211-220. https://doi.org/10.1080/13693780601158779

[43] Rupainoole, R., Calin, G.A., Lopez-Berestein, G. and Sood, A.K. (2016) MicroRNA Deregulation in Cancer Cells and the Tumor Microenvironment. *Cancer Discovery*, **6**, 235-246. https://doi.org/10.1158/2159-8290.CD-15-0893

[44] Mirra, P., Nigro, C., Prevenzano, I., Procopio, T., Leone, A., Raciti, G.A., Andreozzi, F., Longo, M., Fiory, F., Beguinot, F. and Miele, G. (2017) The Role of Mir-190a in Methylglyoxal-Induced Insulin Resistance in Endothelial Cells. *Biochimica et Biophysica Acta*, **183**, 440-449. https://doi.org/10.1016/j.bbadis.2016.11.018

[45] Jiang, J., Xia, Y.M., Liang, Y., Yang, M.L., Zeng, W. and Zeng, X.C. (2018) MiR-190a-5p Participates in the Regulation of Hypoxia-Induced Pulmonary Hypertension by Targeting KLFI5 and Can Serve as a Biomarker of Diagnosis and Prognosis in Chronic Obstructive Pulmonary Disease Complicated with Pulmonary Hypertension. *International Journal of COPD*, **13**, 3777-3790. https://doi.org/10.2147/COPD.S182504

[46] Yu, Y. and Cao, X.C. (2019) MiR-190-5p in Human Disease. *Cancer Cell International*, **19**, 257. https://doi.org/10.1186/s12935-019-0984-x

[47] Shi, J.C., Zhou, T. and Chen, Q. (2022) Exploring the Expanding Universe of Small RNAs. *Nature Cell Biology*, **24**, 415-423. https://doi.org/10.1038/s41556-022-00880-5

Supplemental Material

Table S1. Information of predicted siRNAs in *Penicillium digitatum*.

https://pan.baidu.com/s/17SWymES5oXVr-Zu4LNgifw?pwd=kpf8

Table S2. Predicted target genes of miRNAs in *Penicillium digitatum* using TAPIR software.

Name	Target id	TAPIR score	TAPIR MEF	Pathway	NR ID	Description
Pdmir4	PDIP_84490	4.5	−40	K11262	XP_016603201.1	Acetyl-coenzyme A carboxyltransferase, N-terminal
Pdmir4	PDIP_18360	0	−56	K08744	XP_014537527.1	hypothetical protein
Pdmir5	PDIP_18360	0	−55.1	K08744	XP_014537527.1	hypothetical protein
Pdmir6	PDIP_37860	5	−37.6	K20305	XP_014535618.1	hypothetical protein
Pdmir8	PDIP_54380	5	−32.2	K01183	XP_014534431.1	hypothetical protein
Pdmir8	PDIP_49280	5	−40.4	K19069	XP_014533922.1	hypothetical protein
Pdmir8	PDIP_41050	5	−26.5	K19787	XP_014535096.1	hypothetical protein
Pdmir8	PDIP_85770	5	−28.3	K11244	XP_014530626.1	hypothetical protein
Pdmir8	PDIP_88350	5	−28.8	K03032	XP_014530506.1	26S proteasome regulatory subunit Rpn2, putative
Pdmir8	PDIP_82750	4	−32.2	K15419	XP_014532432.1	Mycocerosic acid synthase
Pdmir8	PDIP_37370	5	−29.4	K19589	XP_014535569.1	hypothetical protein
Pdmir8	PDIP_28910	5	−28.7	K12860	XP_014536352.1	Meiotic sister chromatid recombination protein Ish1/Msc1, putative
Pdmir8	PDIP_40740	4.5	−33.7	K19564	XP_014535065.1	hypothetical protein
Pdmir8	PDIP_14000	5	−29	K12200	OGE50260.1	hypothetical protein
Pdmir8	PDIP_39420	4	−29.8	K03293	XP_016597308.1	Amino acid/polyamine transporter I
Pdmir8	PDIP_80840	2	−38	K05533	XP_014532241.1	hypothetical protein PDIP_80840
Pdmir8	PDIP_17510	5	−29.1	K18423	OQD86217.1	hypothetical protein
Pdmir8	PDIP_20660	4.5	−32	K12232	XP_014537241.1	Ubiquitin-protein ligase (Hul4)
Pdmir12	PDIP_52670	4	−28.4	K04728	XP_014534261.1	hypothetical protein PDIP_52670
Pdmir12	PDIP_19220	4.5	−28.9	K15418	EKV11465.1	Polyketide synthase, putative
Pdmir12	PDIP_07040	5	−34.6	K20121	XP_014538089.1	hypothetical protein
Pdmir12	PDIP_20800	5	−29.7	K14567	XP_014537255.1	Small nucleolar ribonucleoprotein complex subunit Utp14
Pdmir12	PDIP_63510	5	−28.8	K17648	XP_014533577.1	Lipase, putative
Pdmir12	PDIP_03530	5	−32.6	-	XP_014539102.1	BZIP transcription factor, putative
Pdmir12	PDIP_46000	5	−24.5	K01907	XP_014534889.1	Acetoacetyl-CoA synthase
Pdmir12	PDIP_85500	5	−33.8	K02885	KZN92727.1	Translational activator
Pdmir12	PDIP_71050	5	−29.4	K09241	XP_016593745.1	Transcription factor, fungi
Pdmir12	PDIP_35510	5	−28.1	K08793	XP_014535383.1	Protein kinase, putative

Continued

Pdmir12	PDIP_49080	5	−26.7	K13100	XP_014533902.1	hypothetical protein
Pdmir12	PDIP_23840	5	−27.7	K14950	XP_014536865.1	Cation transporting ATPase, putative
Pdmir12	PDIP_44010	NA	NA	K03218	XP_014534691.1	hypothetical protein
Pdmir12	PDIP_37330	5	−31.6	K01277	XP_014535565.1	Efflux pump antibiotic resistance protein, putative
Pdmir12	PDIP_33350	5	−27.3	K15458	XP_014535939.1	hypothetical protein
Pdmir12	PDIP_68600	5	−27.6	K03064	XP_016596476.1	ATPase, AAA-type, core
Pdmir12	PDIP_77160	5	−26.9	K09885	XP_014531873.1	Aquaporin
Pdmir12	PDIP_73730	5	−30.9	K15440	XP_014531530.1	TRNA-specific adenosine deaminase, putative
Pdmir13	PDIP_18360	0	−65.8	K08744	XP_014537527.1	hypothetical protein

NA: not applicable; MFE: minimum free energy; NR: non-redundant database.